Electronic Supplementary Material (ESI) for MedChemComm.

Synthesis, characterization and biological application of 5-quinoline 1,3,5-trisubstituted pyrazole based platinum(II) complexes

Miral V. Lunagariya[a], Khyati P. Thakor[a], Reena R. Varma[a], Bhargav N. Waghela[b], Chandramani Pathak[b] and Mohan N. Patel[a]*

[a]*Department of Chemistry, Sardar Patel University,*

Vallabh Vidyanagar–388 120, Gujarat, India.

Corresponding author. Tel.: +91 2692 226856

E-mail: jeenen@gmail.com

[b] *Department of Cell Biology,*

School of Biological Sciences and Biotechnology,

Indian Institute of Advanced Research,

Koba Institutional Area, Gandhinagar-382007,

Gujarat, India Tel: +91-79-30514245

Supplementary material 1: ^{1}H NMR spectra of the ligands **($L^1 – L^5$)** and platinum(II) complexes **(I-V)**

2-Chloro-3-(3-(5-chlorothiophen-2-yl)-1-phenyl-4,5-dihydro-1*H*-pyrazol-5-yl)quinoline (L^1)

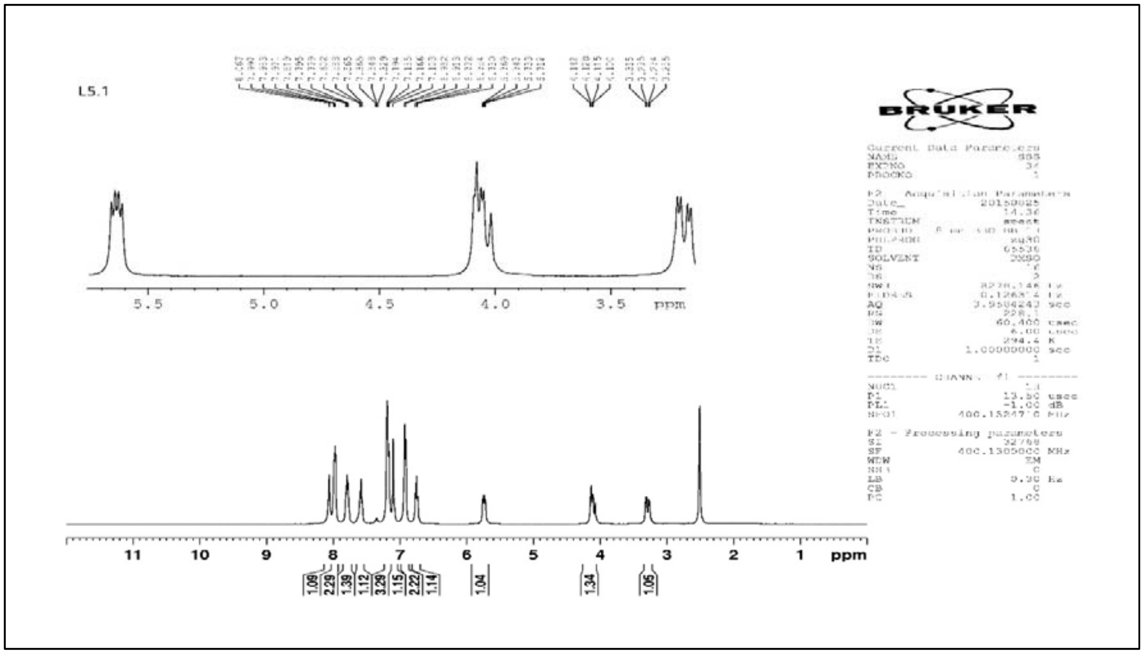

2-Chloro-3-(3-(4-methylthiophen-2-yl)-1-phenyl-4,5-dihydro-1*H*-pyrazol-5-yl)quinoline (L^2)

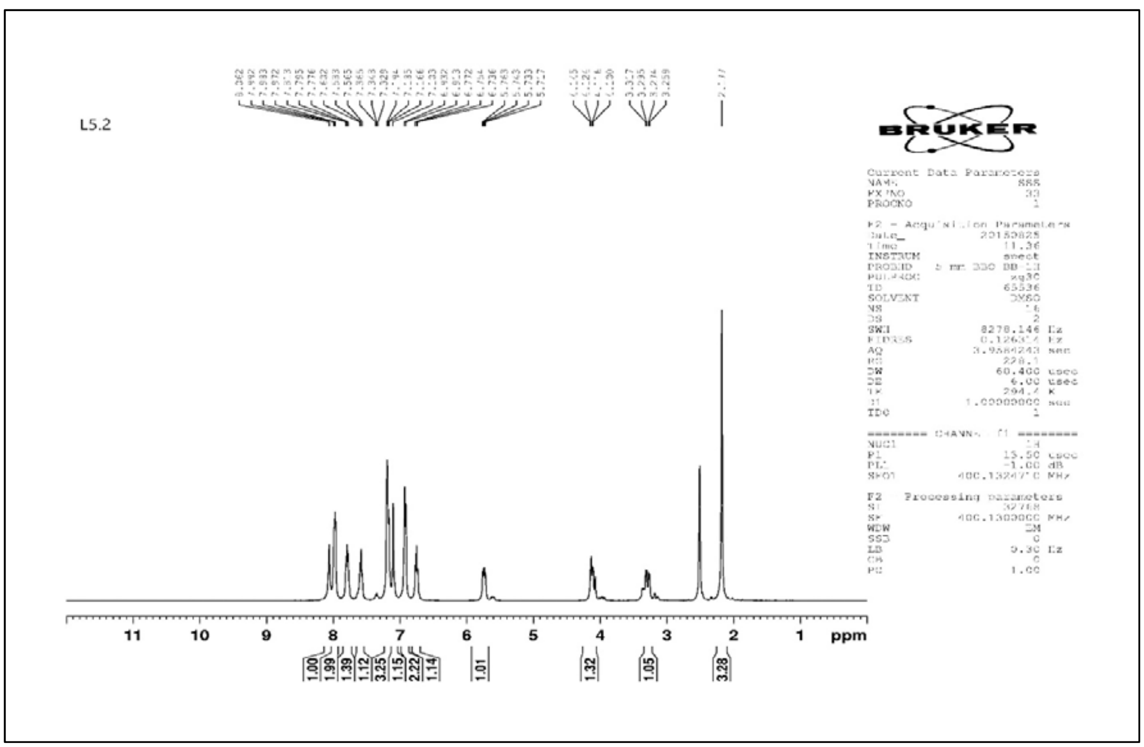

3-(3-(5-Bromothiophen-2-yl)-1-phenyl-4,5-dihydro-1*H*-pyrazol-5-yl)-2-chloroquinoline (L^3)

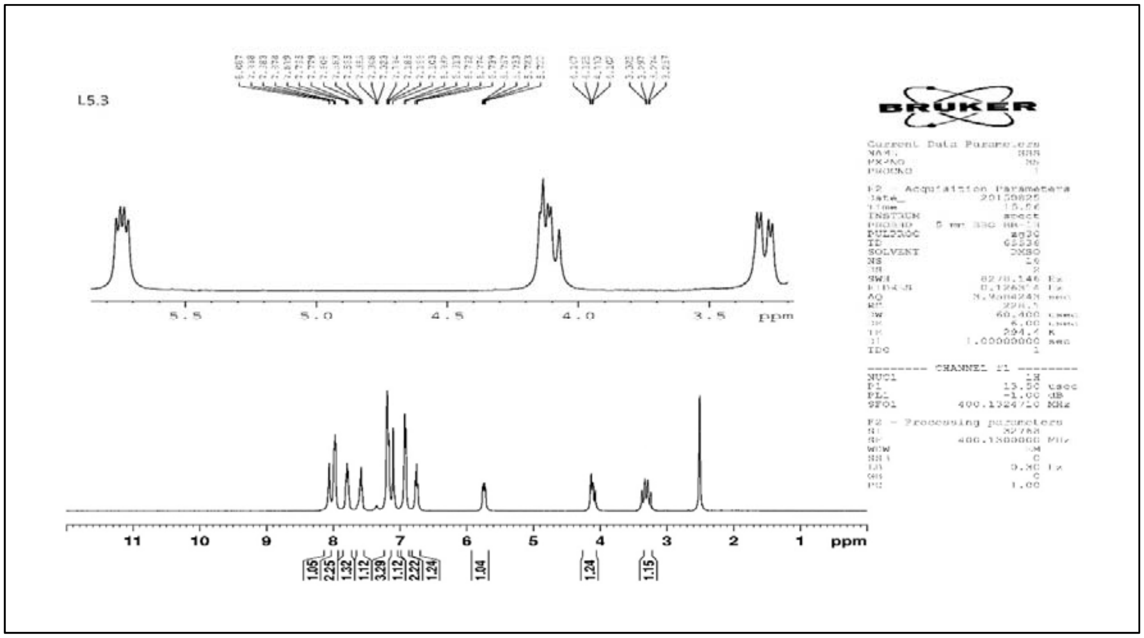

3-(3-(3-Bromothiophen-2-yl)-1-phenyl-4,5-dihydro-1*H*-pyrazol-5-yl)-2-chloroquinoline (L^4)

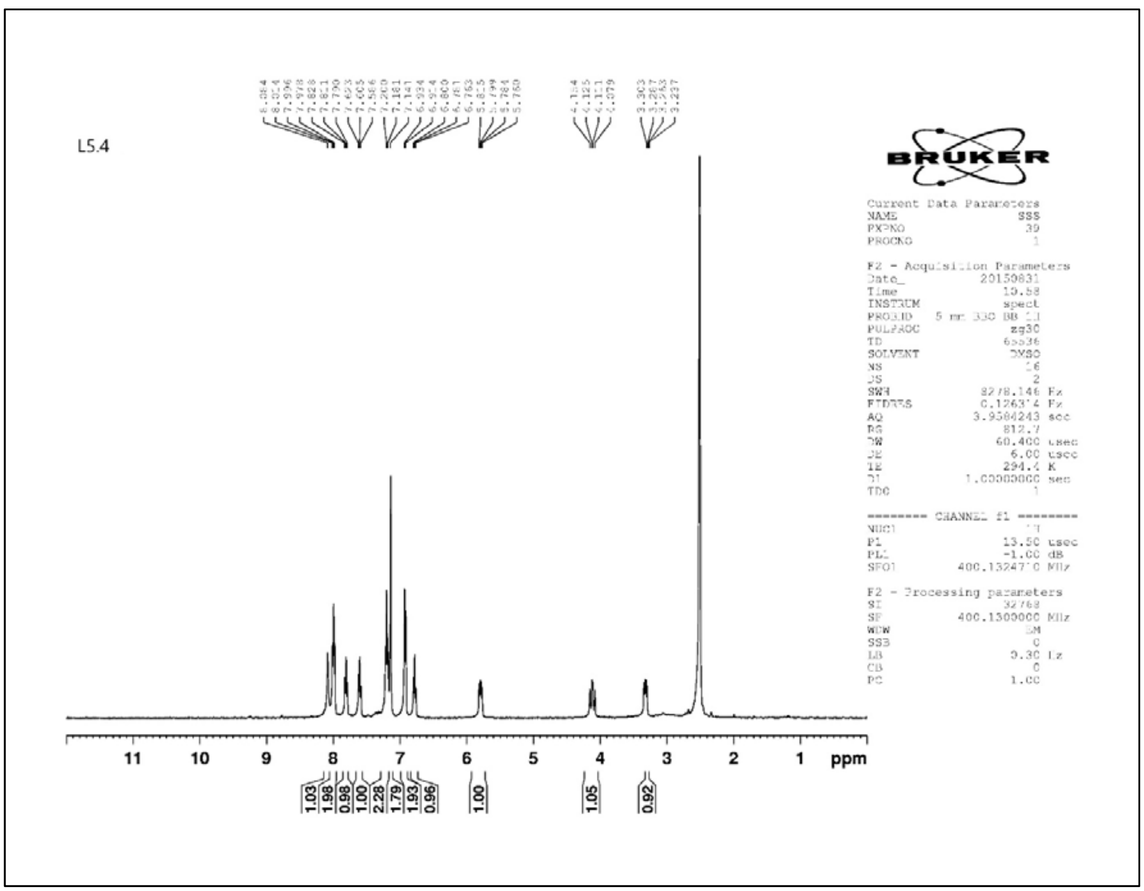

2-Chloro-3-(1-phenyl-3-(thiophen-2-yl)-4,5-dihydro-1*H*-pyrazol-5-yl)quinoline (L[5])

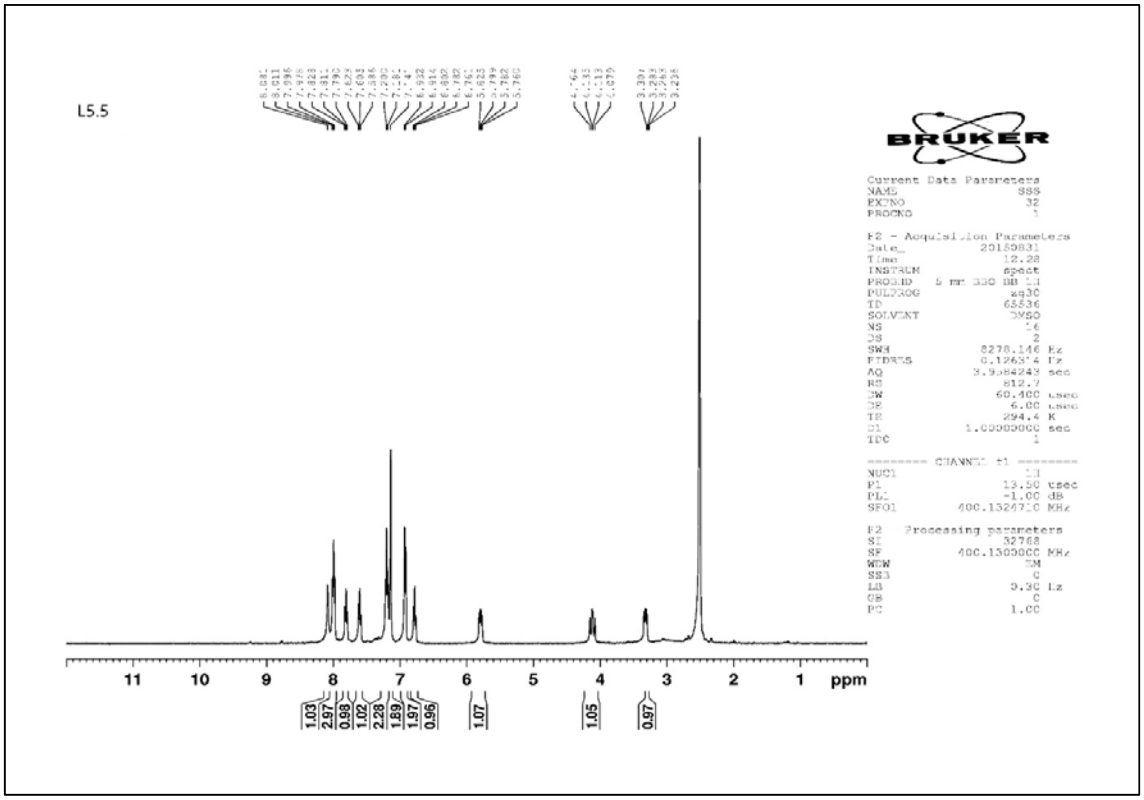

Complex [Pt(L[1])Cl$_2$] (I)

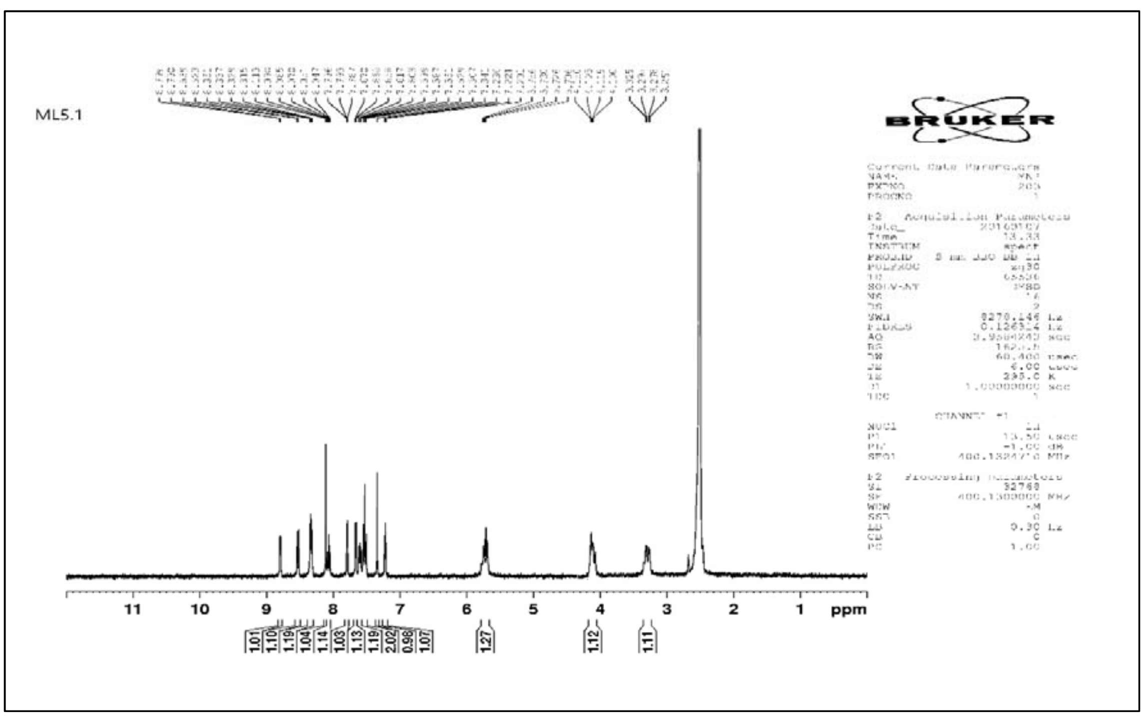

Complex $[Pt(L^2)Cl_2]$ (II)

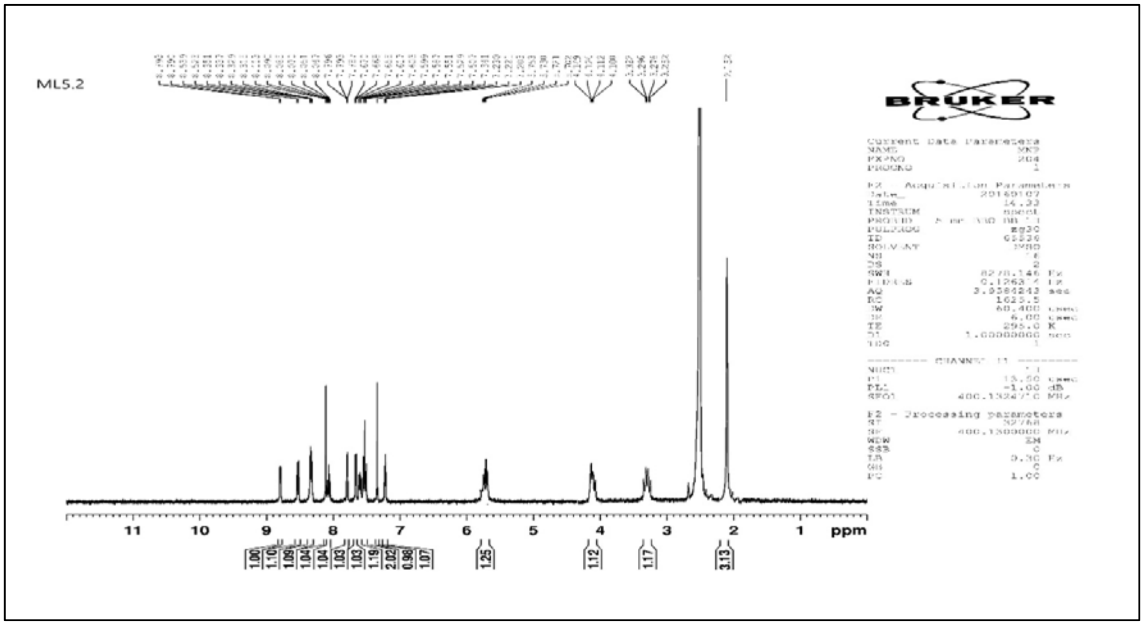

Complex [Pt(L^3)Cl_2] (III)

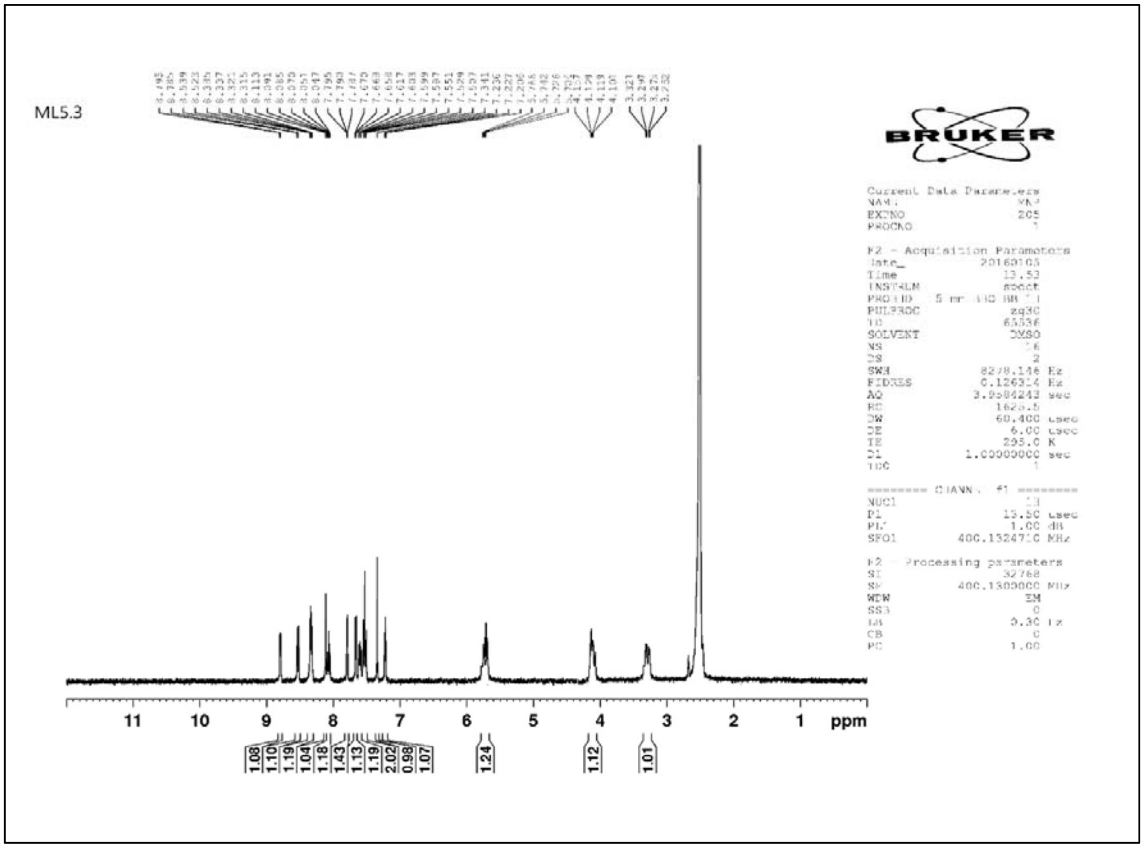

Complex [Pt(L^4)Cl_2] (IV)

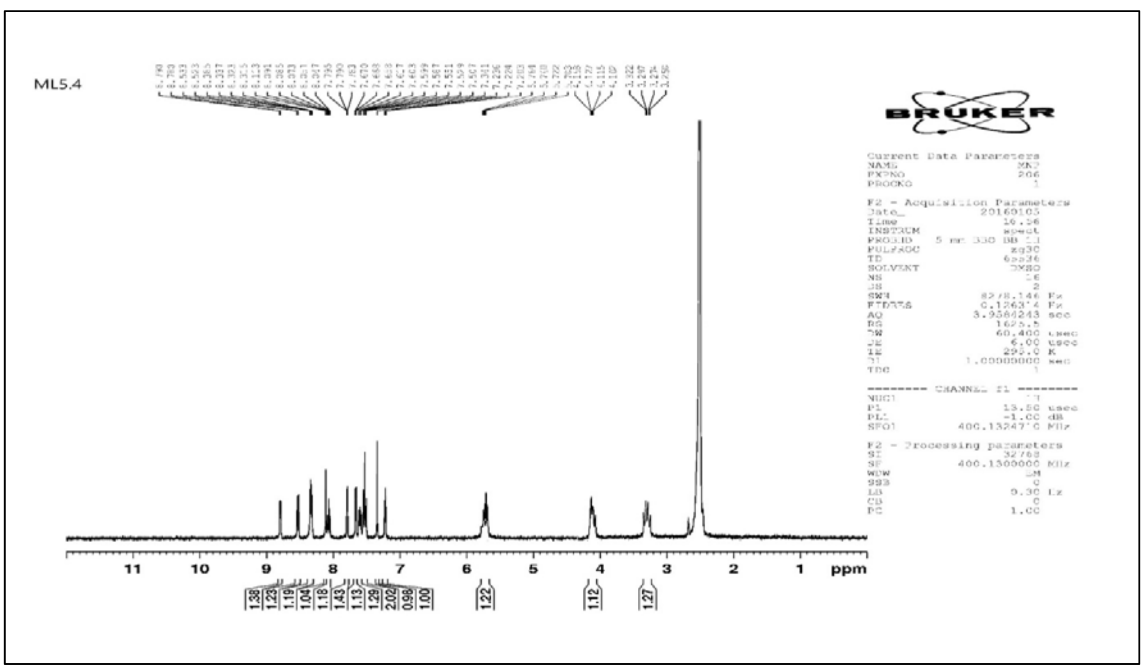

Complex [Pt(L^5)Cl_2] (V)

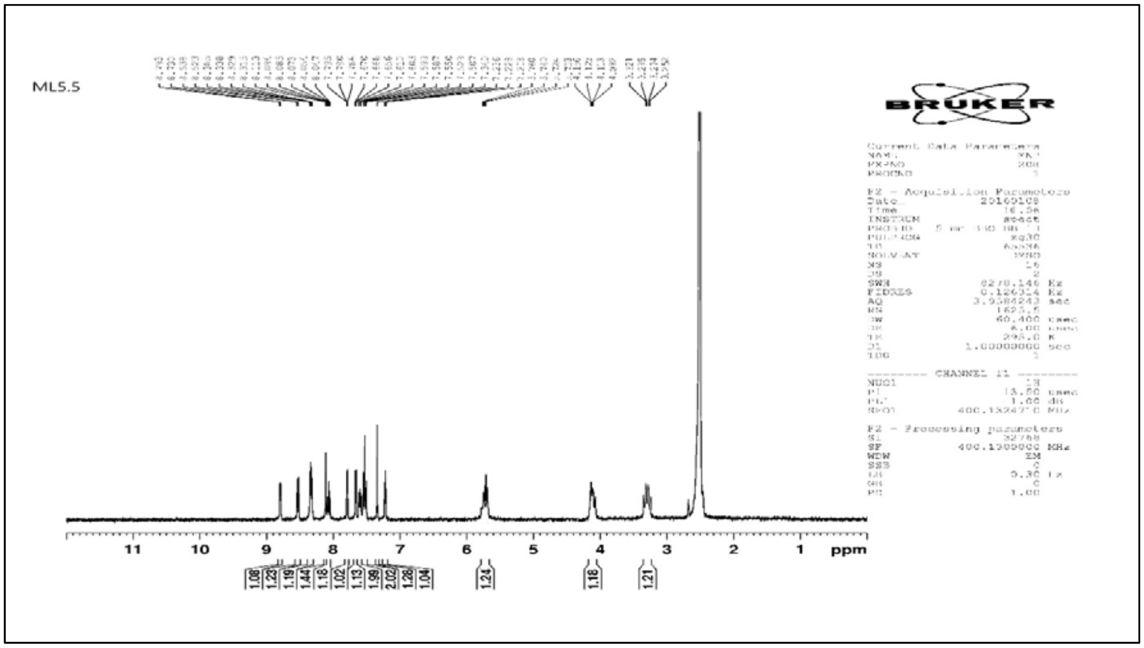

Supplementary 2: ^{13}C NMR spectra of the ligands (L^1-L^5) and platinum(II) complexes (I - V)

2-Chloro-3-(3-(5-chlorothiophen-2-yl)-1-phenyl-4,5-dihydro-1*H*-pyrazol-5-yl)quinoline (L^1)

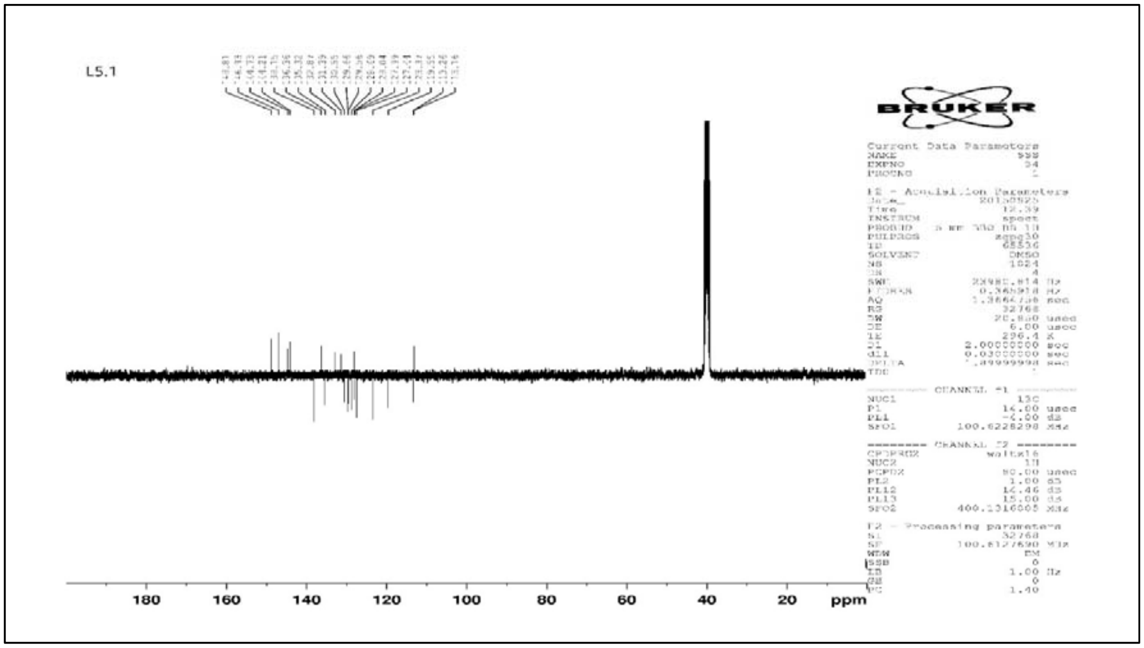

2-Chloro-3-(3-(4-methylthiophen-2-yl)-1-phenyl-4,5-dihydro-1*H*-pyrazol-5-yl)quinoline (L^2)

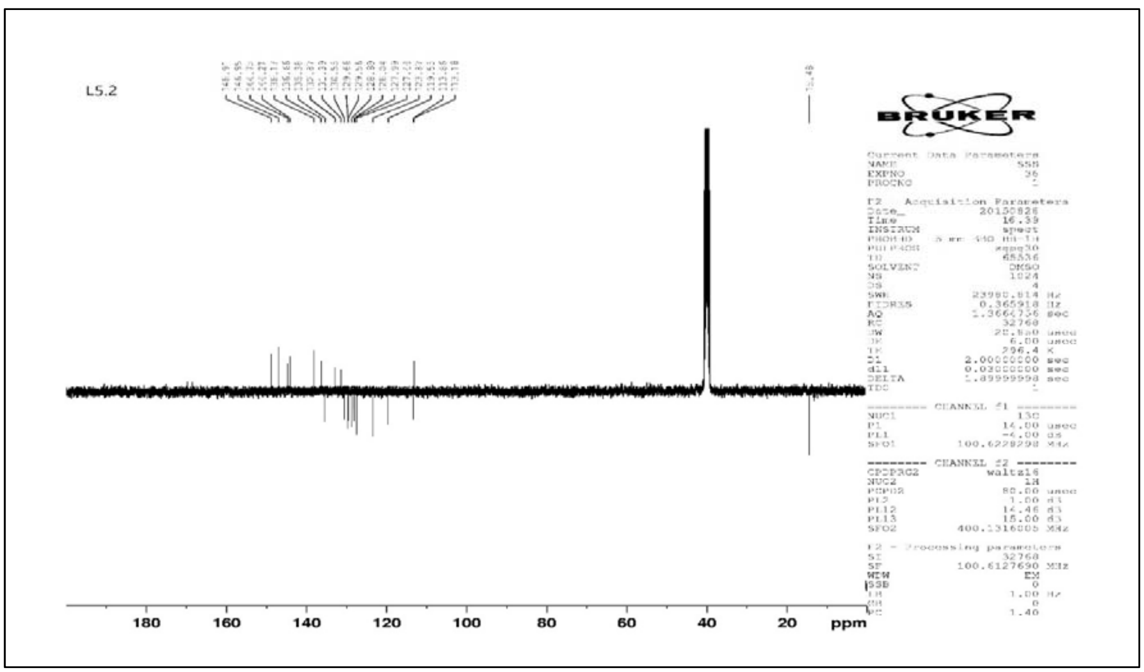

3-(3-(5-Bromothiophen-2-yl)-1-phenyl-4,5-dihydro-1*H*-pyrazol-5-yl)-2-chloroquinoline (L[3])

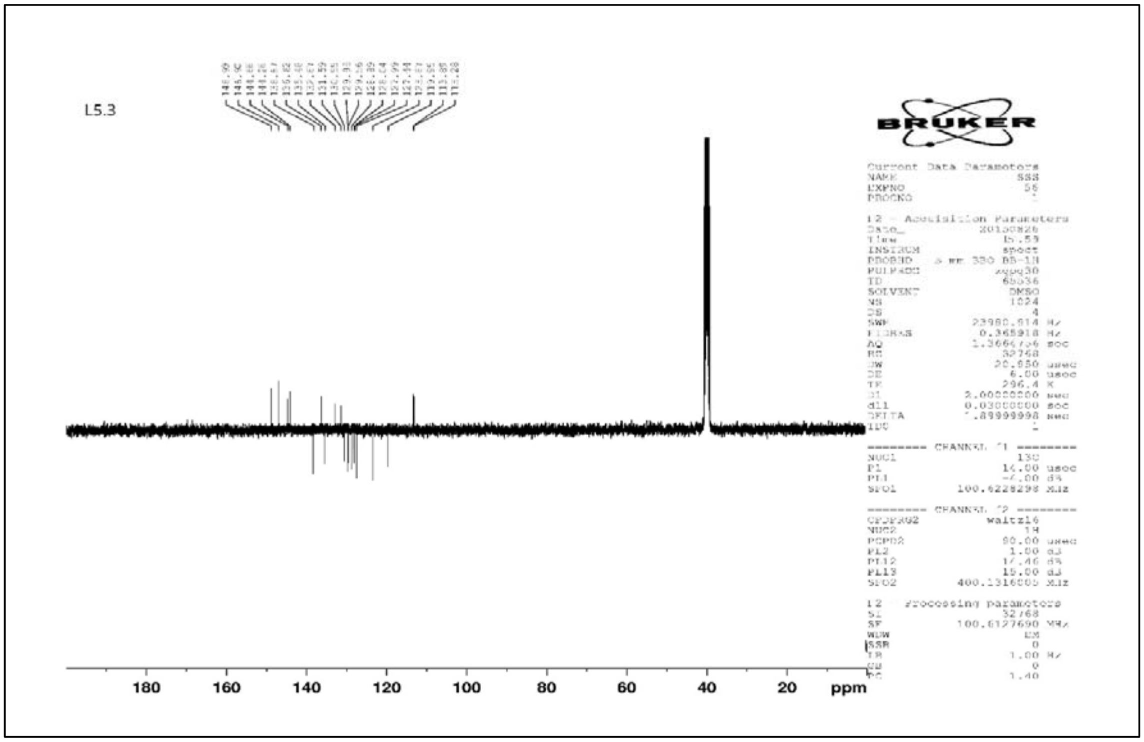

3-(3-(3-Bromothiophen-2-yl)-1-phenyl-4,5-dihydro-1*H*-pyrazol-5-yl)-2-chloroquinoline (L[4])

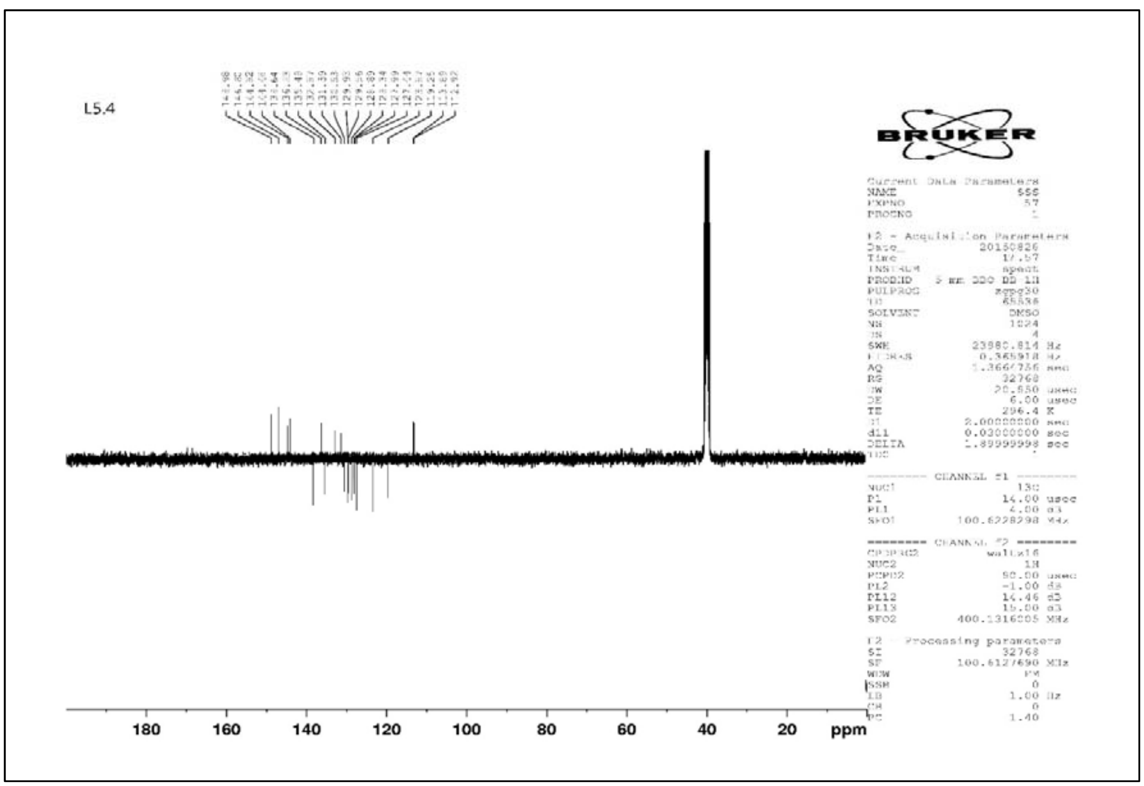

2-Chloro-3-(1-phenyl-3-(thiophen-2-yl)-4,5-dihydro-1*H*-pyrazol-5-yl)quinoline (L[5])

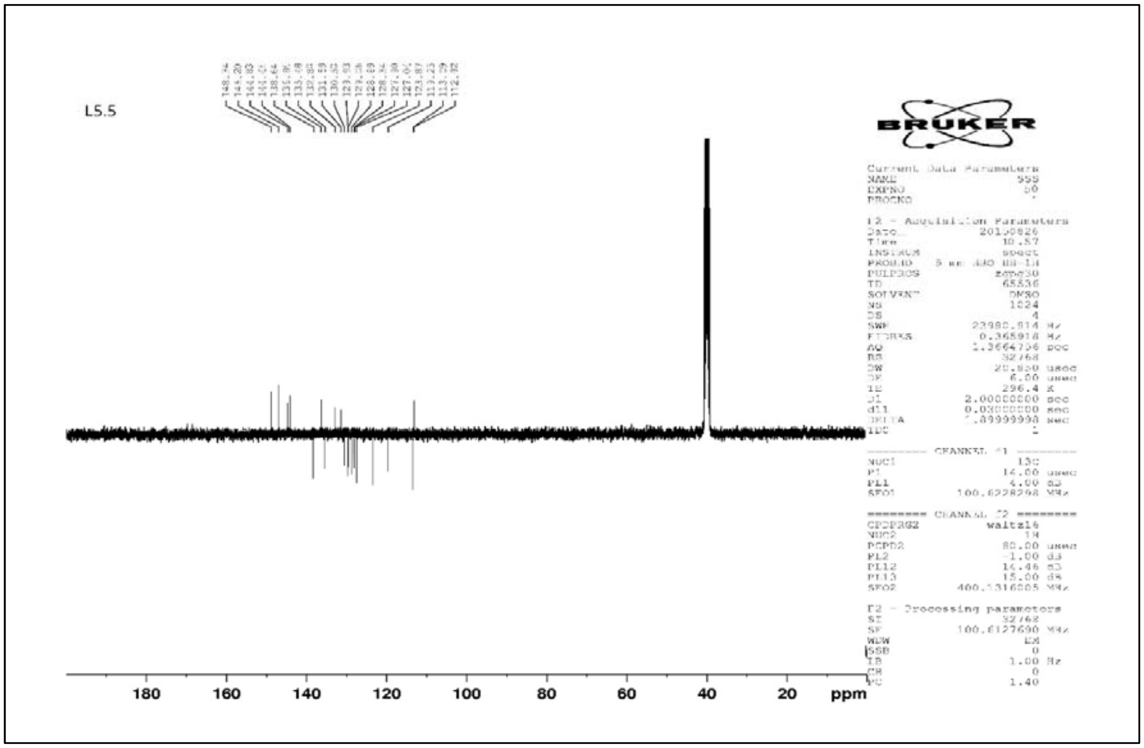

Complex [Pt(L[1])Cl$_2$] (I)

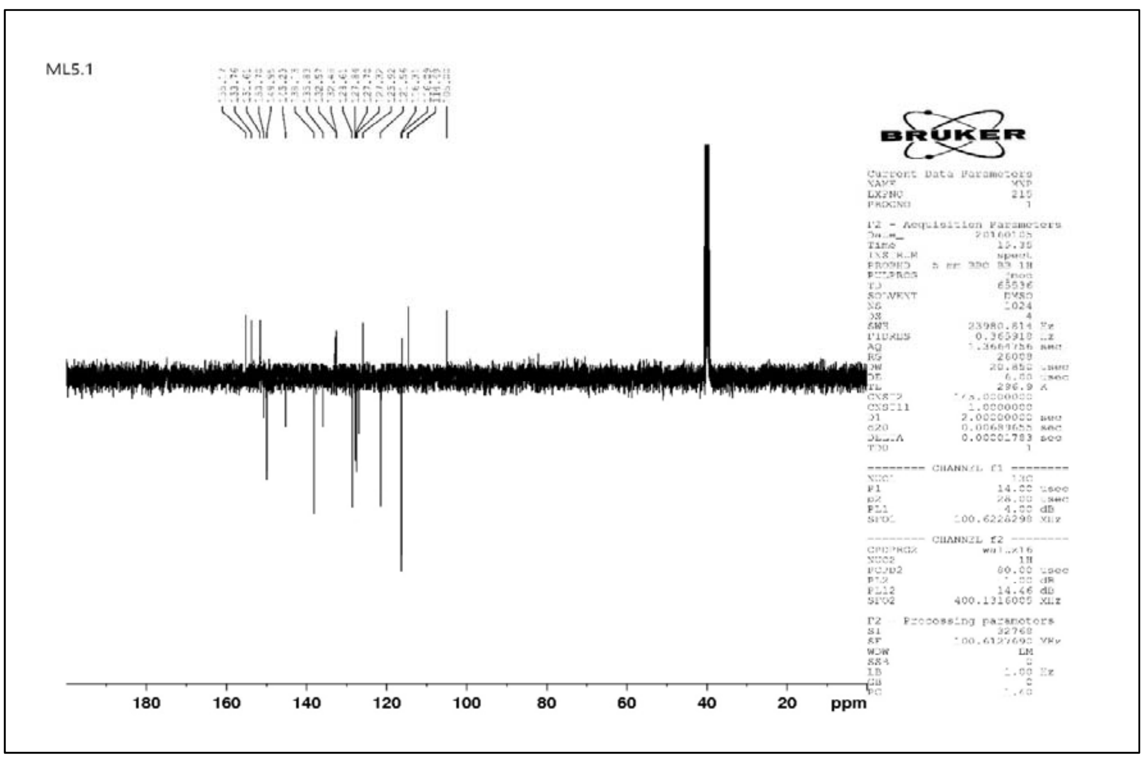

Complex [Pt(L^2)Cl_2] (II)

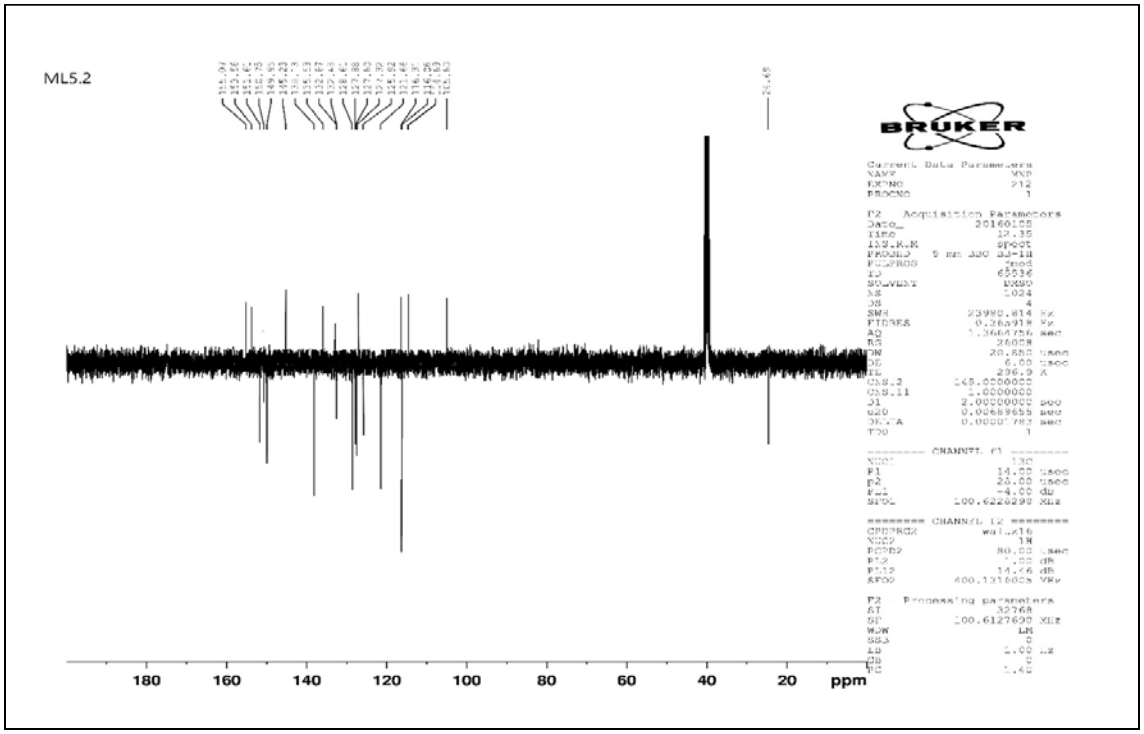

Complex [Pt(L^3)Cl_2] (III)

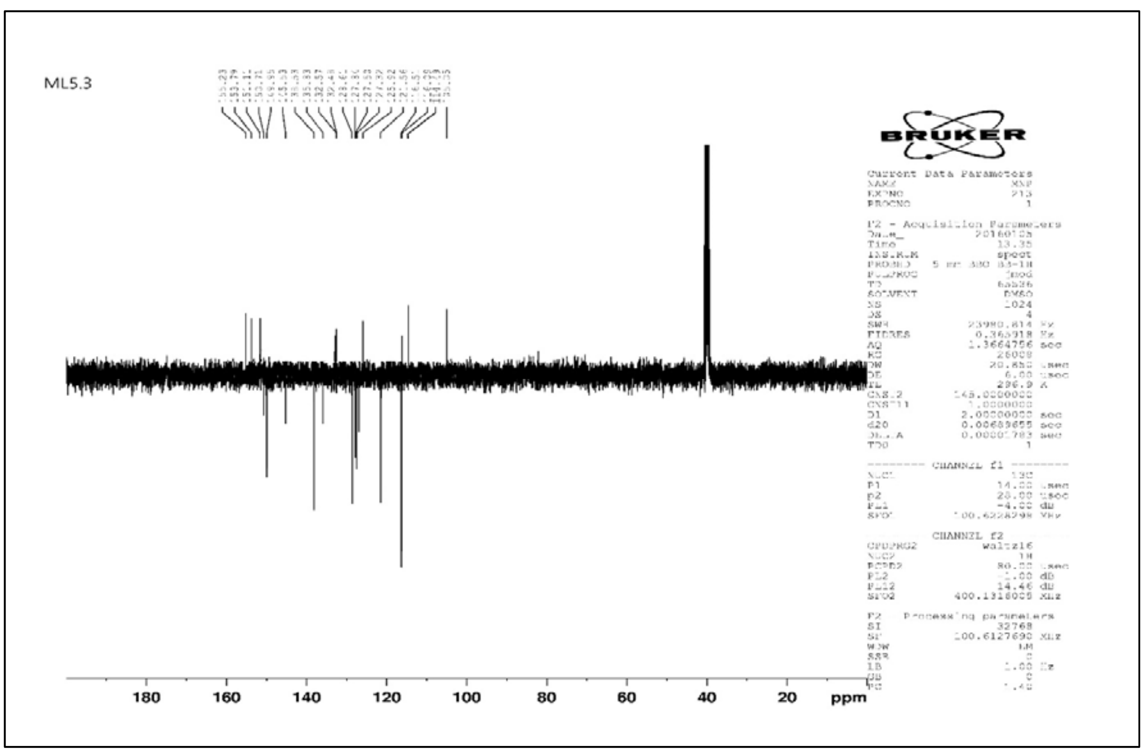

Complex $[Pt(L^4)Cl_2]$ (IV)

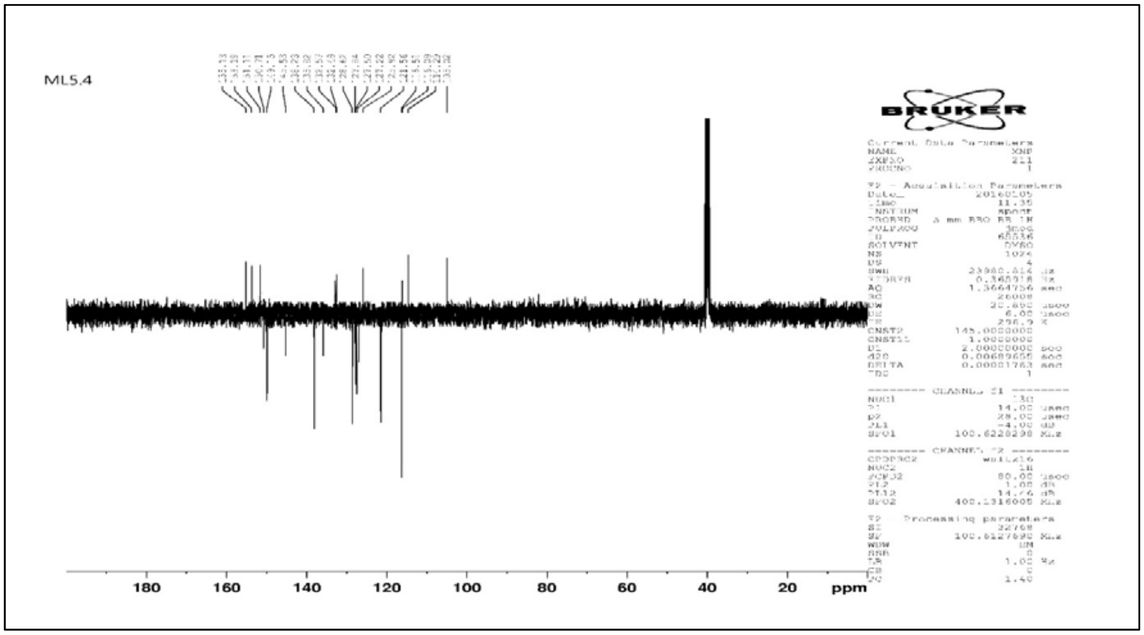

Complex $[Pt(L^5)Cl_2]$ (V)

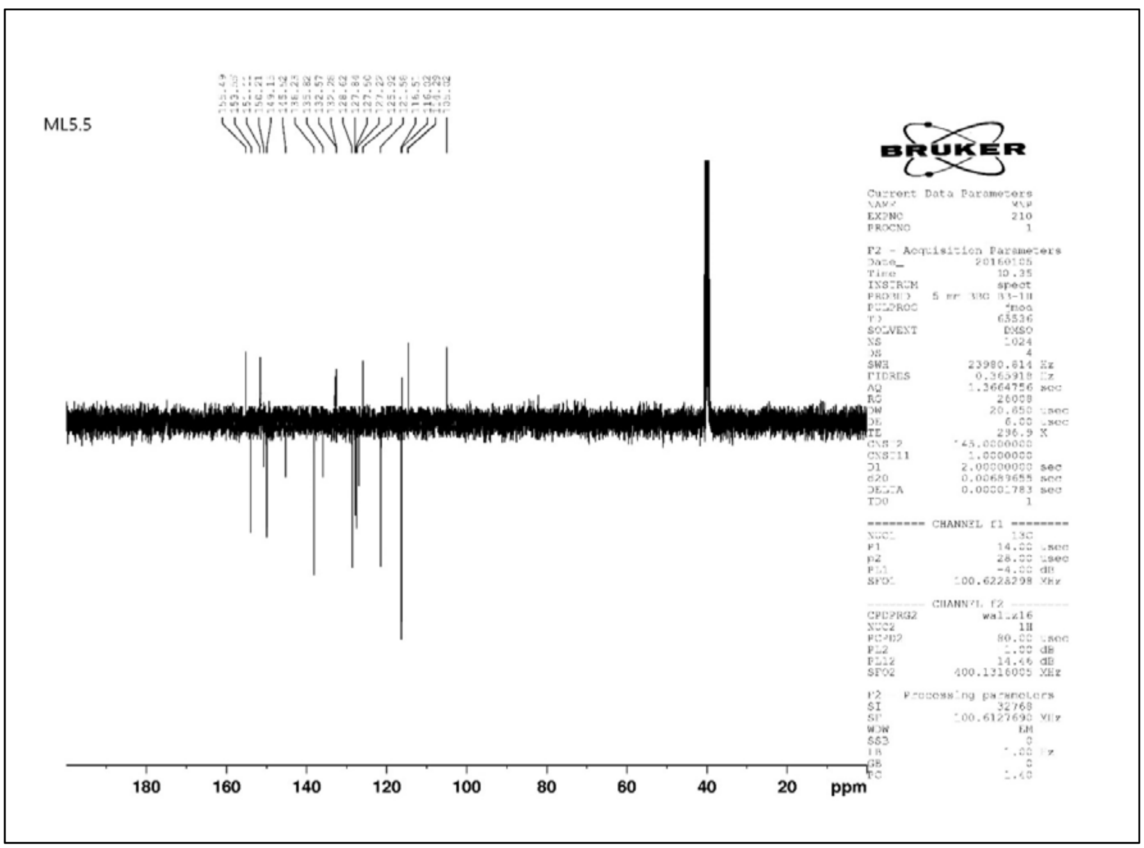

Supplementary material 3:

Compounds	ν(=C-H)ar cm-1	ν(C=N) cm-1	ν(C-H)banding cm-1	ν(C=C)conjugated alkenes cm-1	ν(C-S-C)stre. (thiophene ring) cm-1	ν(Ar-H)2 adjacent hydrogen cm-1	ν(N-Pt) cm-1	ν(S-Pt) cm-1
L^1	3039	1596 - 1558	1388	1496 -1458	1041	786 – 678	-	-
L^2	3039	1596 - 1559	1388	1496 -1450	1041	779 – 678	-	-
L^3	3039	1596 - 1559	1388	1496 -1450	1041	779 – 678	-	-
L^4	3039	1596 - 1542	1388	1496 -1458	1042	786 – 678	-	-
L^5	3038	1596 - 1543	1387	1496 -1450	1042	786 – 678	-	-
I	3170	1596 - 1566	1388 - 1326	1504 -1458	1072	779 – 655	524	509
II	3163	1596 - 1566	1380 - 1326	1496 -1473	1072	740 – 686	555	509
III	3170	1596 - 1566	1388 - 1326	1450 - 1504	1070	779 – 655	555	439
IV	3163	1596 - 1566	1388 - 1326	1496 - 1458	1072	779 – 655	555	509
V	3124	1604 - 1566	1396 - 1326	1504 - 1465	1049	756 – 671	563	439

ESI Table 1. FT-IR spectral data of the synthesized ligands **(L^1–L^5)** and platinum(II) complexes **(I - V)**

Supplementary material 4: Mass fragmentation pattern graph of platinum(II) complex **(I)**

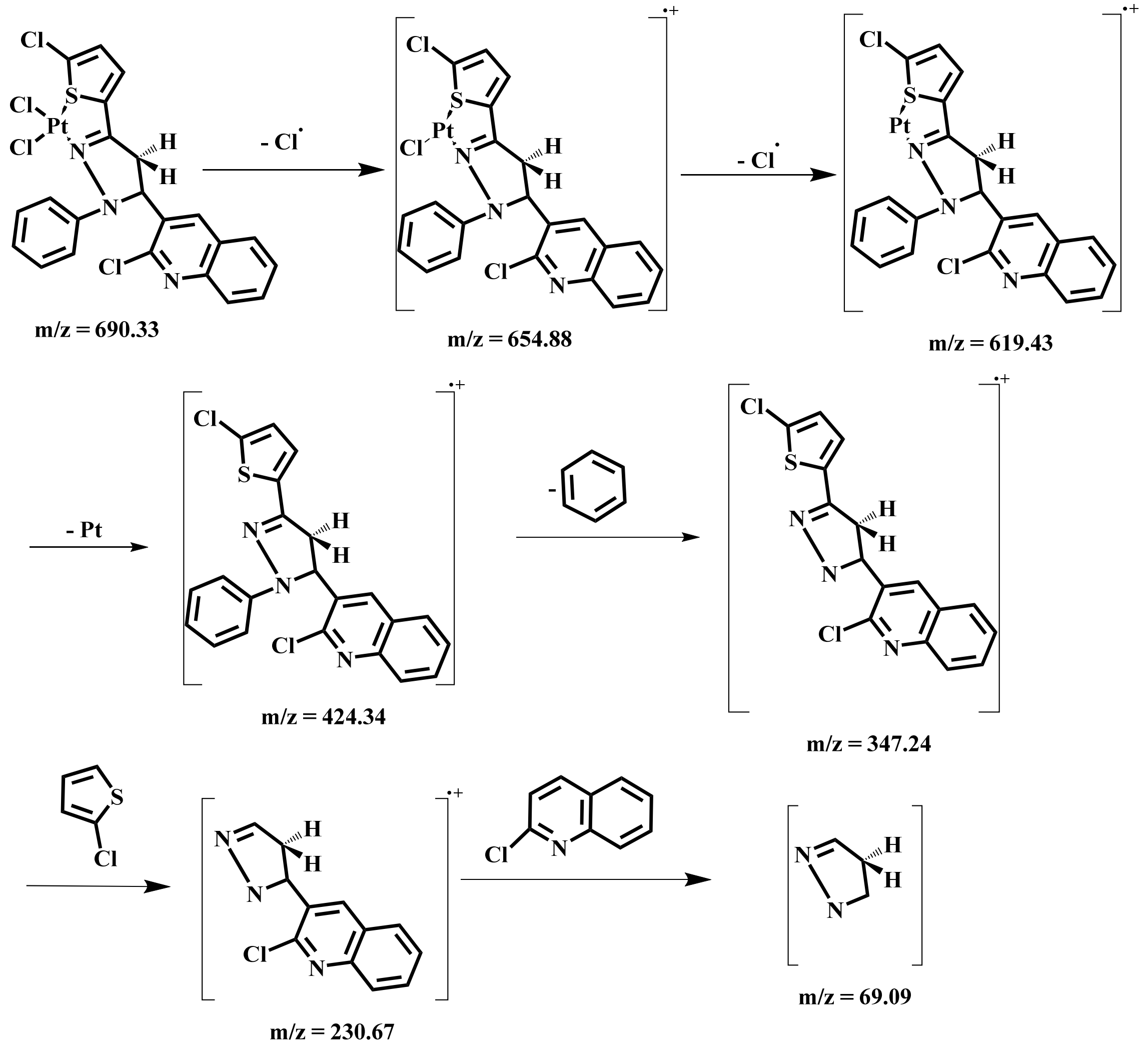

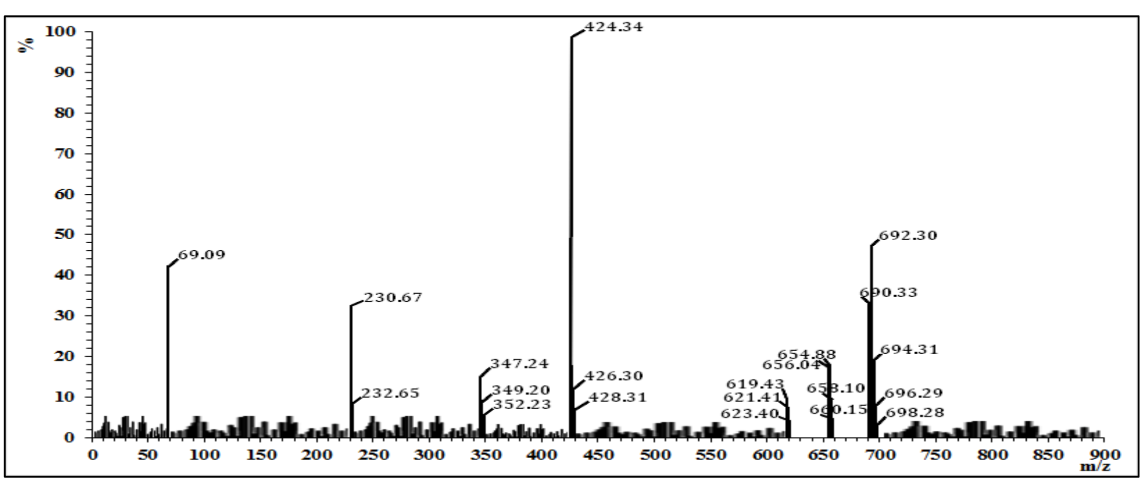

Supplementary material 5: Minimum inhibitory concentration (MIC) values of the ligands **(L^1-L^5)** and platinum(II) complexes **(I - V)**. Error bar are a representation of the experiment repeated in three times and STD ± 5%.

	Gram(+ve) microorganism		Gram(-ve) microorganism		
Compounds	***S. Aureus***	***B. subtilis***	***S. marcescens***	***P. aeruginosa***	***E. coli***
K_2PtCl_4	2792	2688	2756	2956	3289
L^1	**250**	**235**	**219**	**232**	**221**
L^2	286	290	280	282	284
L^3	**247**	**237**	**220**	**235**	**225**
L^4	**265**	**270**	**260**	**269**	**255**
L^5	260	250	262	265	250
I	**38**	**40**	**42**	**50**	**45**
II	90	85	75	88	78
III	**42**	**45**	**46**	**55**	**48**
IV	**70**	**75**	**82**	**80**	**85**
V	72	77	85	90	92

Supplementary material 6: *In vitro* brine shrimp cytotoxicity of the cisplatin, transplatin, platinum(II) complexes (I-V) and ligands (L^1-L^5).

Compounds	**LC_{50} µg/mL**
L^1	79.25
L^2	94.84
L^3	80.9
L^4	89.12
L^5	100
Cisplatin	3.133
Transplatin	14.45
I	6.295
II	7.44
III	6.44
IV	6.561
V	8.189

Supplementary material 7: The percentage viability of compounds at different concentrations with error uncertainty in the value ±5%.

Compounds	20 µM	40 µM	60 µM	80 µM	100 µM
L^1	80	77	74	71	68
L^2	96	92	90	87	76
L^3	85	83	80	76	73
L^4	87	85	81	79	74
L^5	91	87	85	81	75
Cisplatin	59	56	49	44	37
trans platin	62	57	52	48	43
I	55	53	50	47	40
II	66	55	51	46	42
III	57	56	52	49	43
IV	63	60	57	55	50
V	65	63	54	50	47

Supplementary material 8: Molecular docking study of the quinoline substituted-1-*H* pyrazole derivatives ligands (L^1-L^5) and platinum(II) complexes (I-V)

2-Chloro-3-(3-(5-chlorothiophen-2-yl)-1-phenyl-4,5-dihydro-1*H*-pyrazol-5-yl)quinoline (L^1)

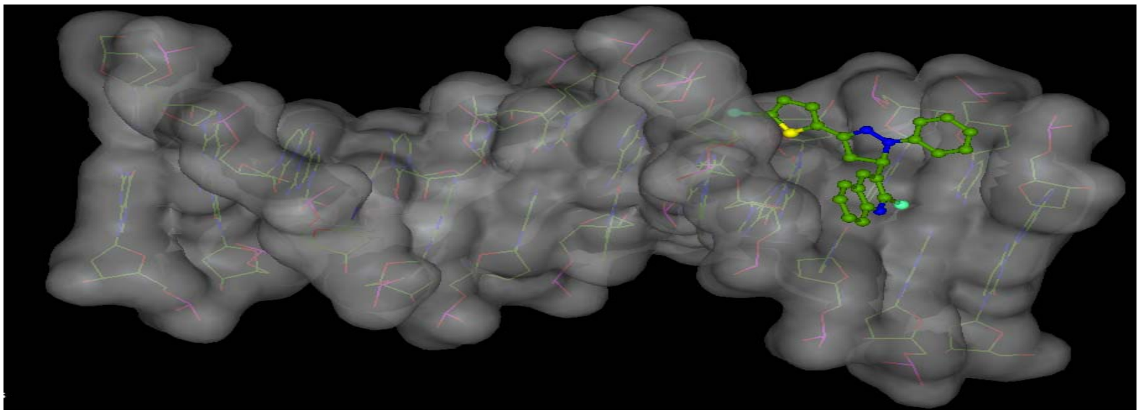

2-Chloro-3-(3-(4-methylthiophen-2-yl)-1-phenyl-4,5-dihydro-1*H*-pyrazol-5-yl)quinoline (L^2)

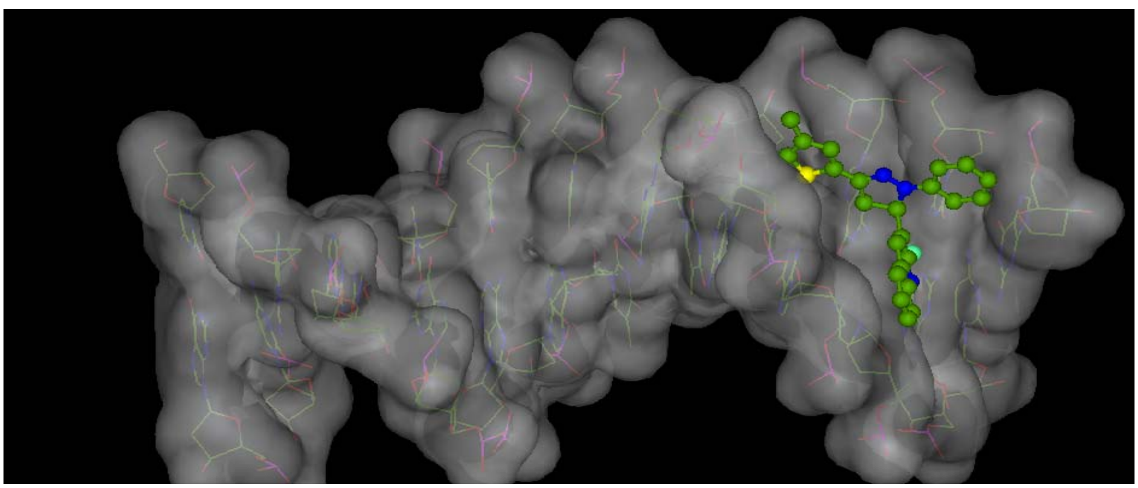

3-(3-(5-Bromothiophen-2-yl)-1-phenyl-4,5-dihydro-1*H*-pyrazol-5-yl)-2-chloroquinoline (L[3])

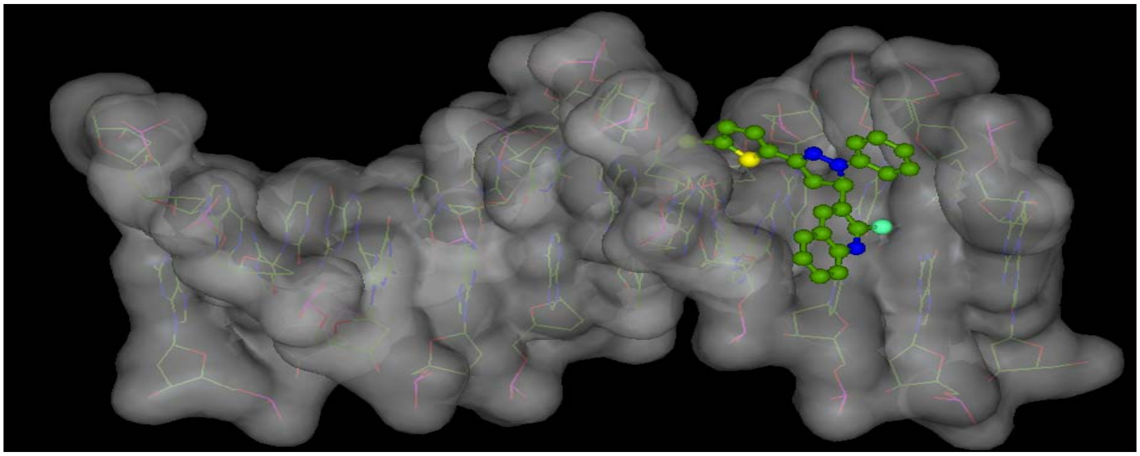

3-(3-(3-Bromothiophen-2-yl)-1-phenyl-4,5-dihydro-1*H*-pyrazol-5-yl)-2-chloroquinoline (L[4])

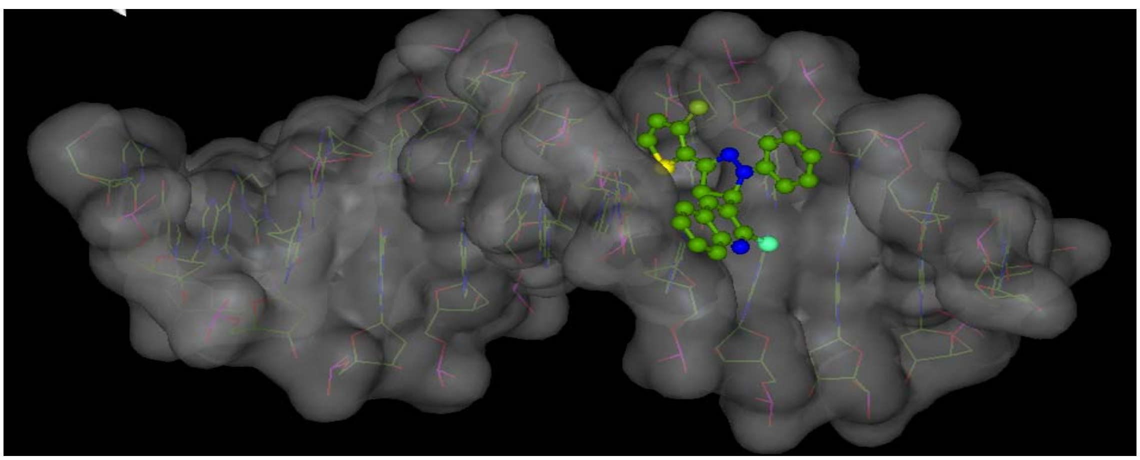

2-Chloro-3-(1-phenyl-3-(thiophen-2-yl)-4,5-dihydro-1*H*-pyrazol-5-yl)quinoline (L[5])

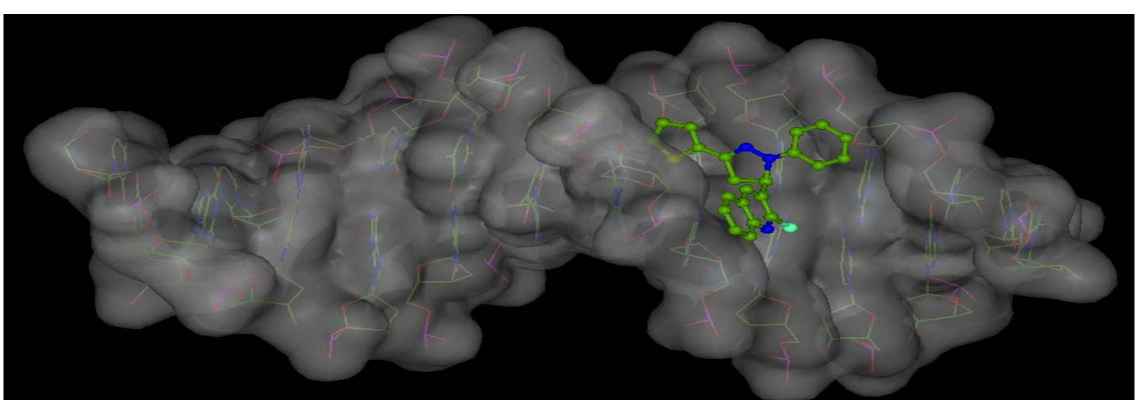

Complex [Pt(L^1)Cl_2] (I)

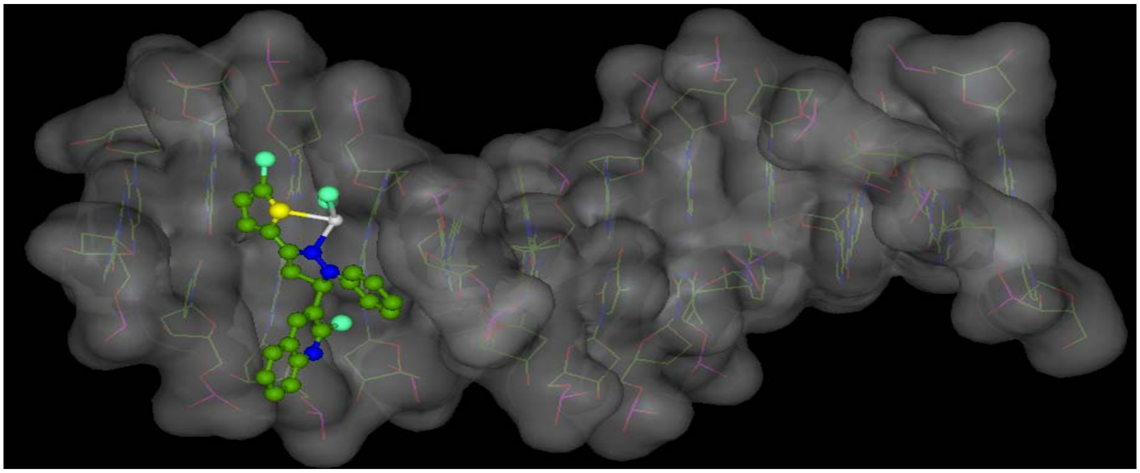

Complex [Pt(L^2)Cl_2] (II)

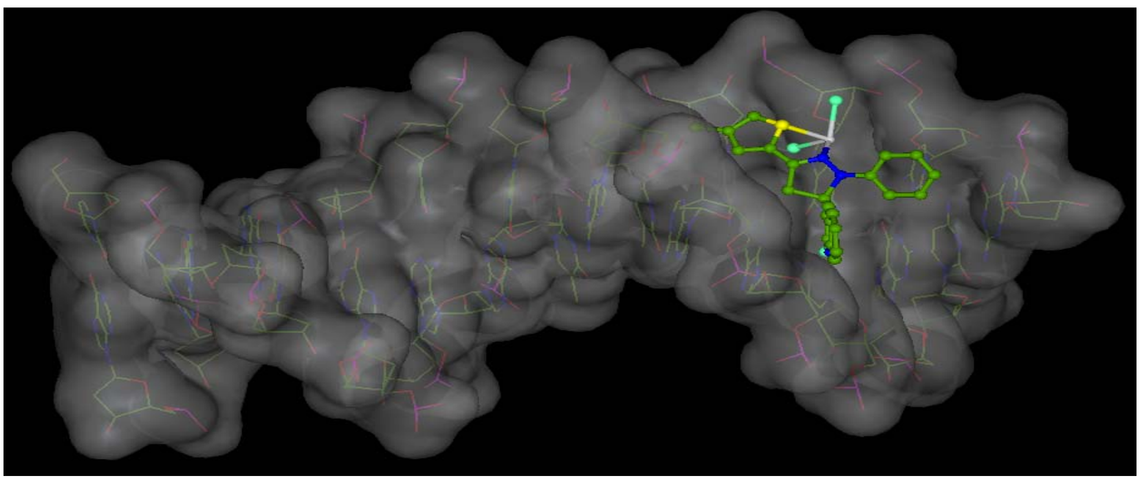

Complex [Pt(L^3)Cl_2] (III)

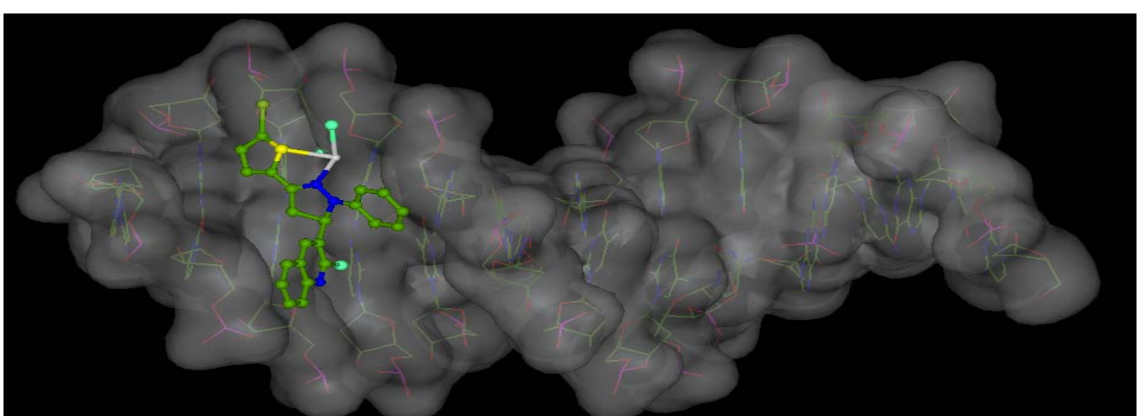

Complex $[Pt(L^4)Cl_2]$ (IV)

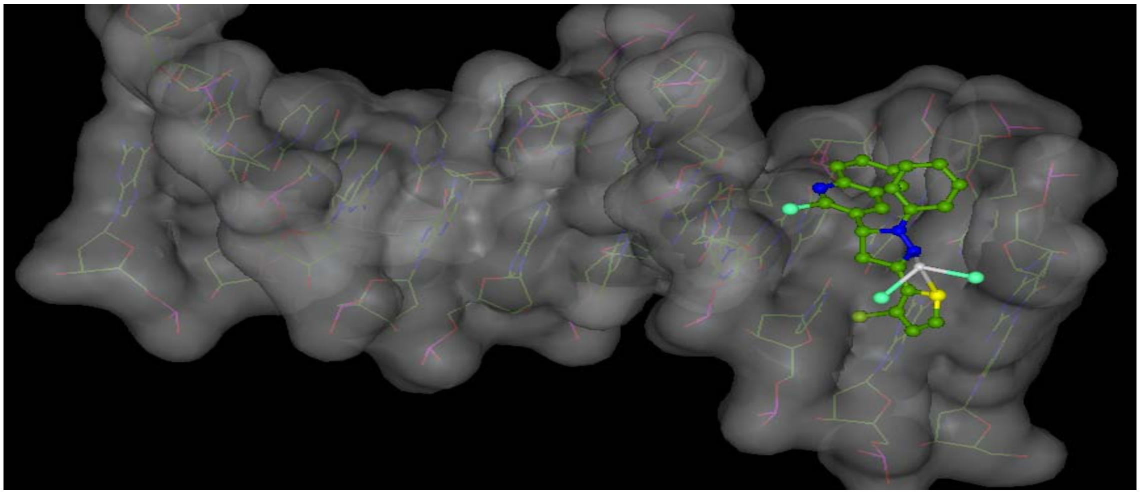

Complex $[Pt(L^5)Cl_2]$ (V)

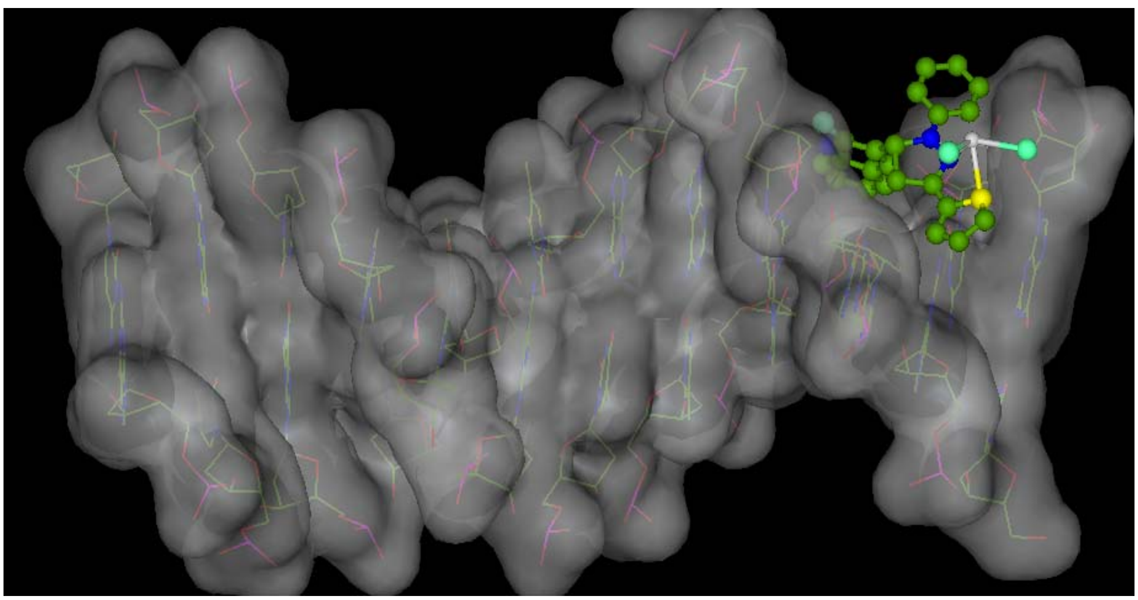

Supplementary material 9: Linear Stern-Volmer quenching constant (K_q), binding sites (n) and association binding constant (K_a) of the platinum(II) complexes **(I-V)** are determined by fluorescence quenching analysis assay.

[Pt(L^1)Cl$_2$] (I)

Volume (μL)	Intensity (CPS) $I_{corr.}$	Intensity (CPS) $I_{obs.}$	I_o/I	$(I_o - I)/I$	$\log(I_o - I/I)$	$Q \times 10^{-6}$ (μM)	log Q	K_q (M^{-1})	K_a (M^{-1})	n	ΔG ($Jmol^{-1}$)
0	74909	74760	1.002	0	-	0	-	1.1×10^2	1.44×10^5	1.2551	-29,435.73
5	73392	73246	1.022	0.022	-1.64385	3.33	-5.47712				
10	72342	72198	1.037	0.037	-1.42534	6.66	-5.17609				
15	69704	69565	1.076	0.076	-1.11452	10	-5				
20	67825	67690	1.106	0.106	-0.97202	13.3	-4.87506				
25	65565	65434	1.144	0.144	-0.83923	16.6	-4.77815				
30	63984	63857	1.173	0.173	-0.76176	20	-4.69897				
35	62139	62015	1.207	0.207	-0.68211	23.3	-4.63202				
40	58310	58194	1.287	0.287	-0.54178	26.6	-4.57403				
45	56404	56291	1.330	0.330	-0.48052	30	-4.52288				
50	55499	55389	1.352	0.352	-0.45293	33.3	-4.47712				

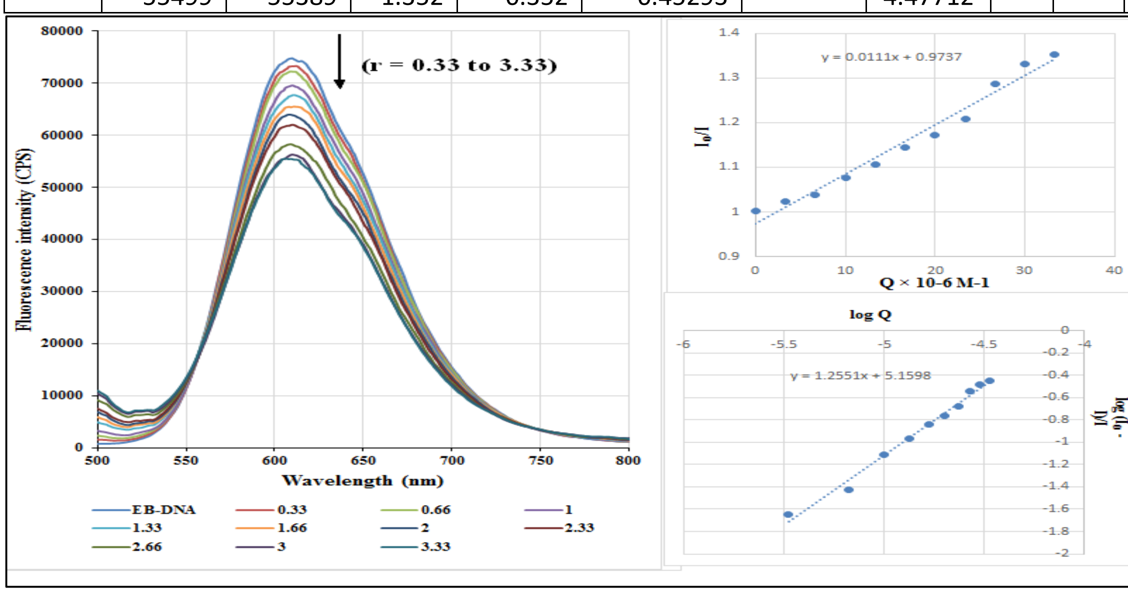

ESI Fig. 1. Fluorescence emission spectra of EB bound to HS-DNA in the presence of complexes (I). [EB] = 33.3 µM, [DNA] = 10 µM; [complex] = (i) 3.33, (ii) 6.66, (iii) 10, (iv) 13.33, (v) 16.66, (vi) 20, (vii) 23.33, (viii) 26.66, (iX) 30, (X) 33.3 µM; λex= 510 nm. The arrows show the intensity changes upon increasing the concentrations of complex. Inset graph: plots of I_o/I vs. [Q], with • for the experimental data points and the full line for the linear fitting of the data. Comparative plot of log[I_o-I/I] versus log[complex] for the titration of HS-DNA EB system with platinum(II) complex (I) in phosphate buffer medium.

[Pt(L^2)Cl_2] (II)

Volume (µL)	Intensity (CPS) $I_{corr.}$	Intensity (CPS) $I_{obs.}$	I_o/I	$(I_o - I)/I$	$\log(I_o - I/I)$	Q × 10^{-6} (µM)	log Q	K_q (M^{-1})	K_a (M^{-1})	n	ΔG($Jmol^{-1}$)
0	68461	68324	1.002	0	-	0	-	2.2× 10^3	0.434 × 10^3	0.844	-14,991.69
5	67901	67766	1.010	0.0102	-1.98914	3.33	-5.47712				
10	67384	67250	1.018	0.0180	-1.74448	6.66	-5.17609				
15	66620	66487	1.029	0.0296	-1.52742	10	-5				
20	66418	66285	1.032	0.0328	-1.48381	13.3	-4.87506				
25	66299	66167	1.034	0.0346	-1.46007	16.6	-4.77815				
30	66010	65879	1.039	0.0391	-1.40677	20	-4.69897				
35	65517	65386	1.047	0.0470	-1.32767	23.3	-4.63202				
40	64664	64535	1.060	0.0608	-1.21588	26.6	-4.57403				
45	64421	64292	1.064	0.0648	-1.18819	30	-4.52288				
50	63175	63049	1.085	0.0858	-1.06631	33.3	-4.47712				

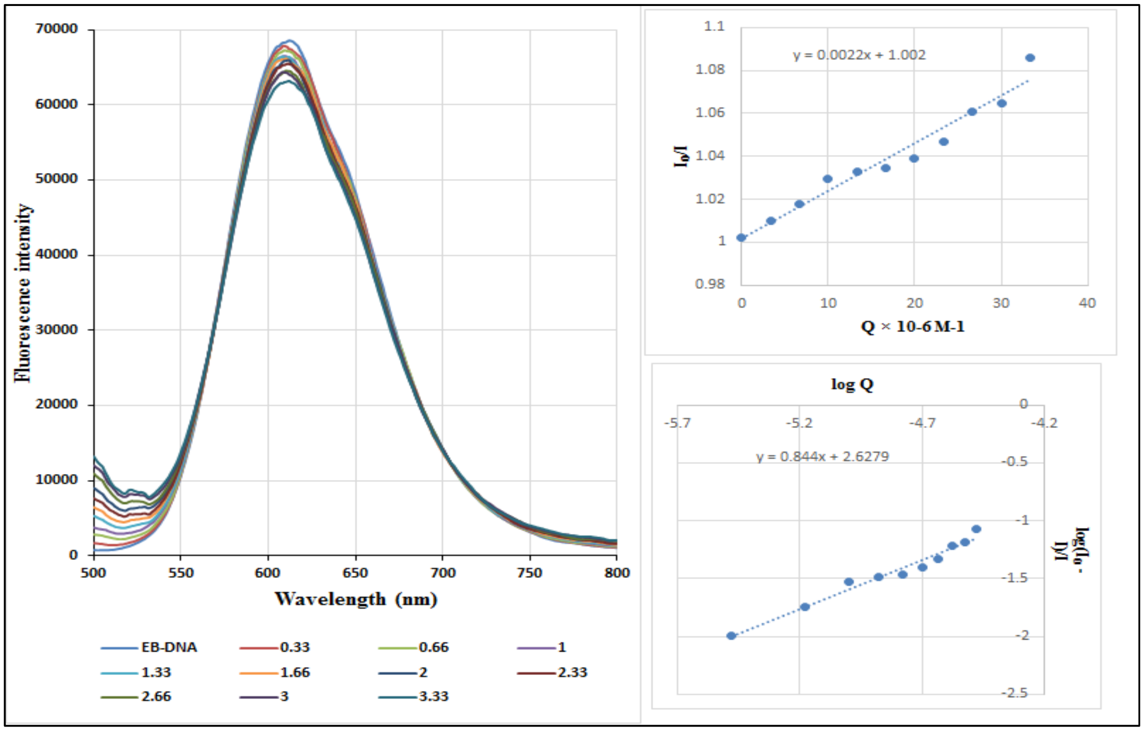

ESI Fig. 2. Fluorescence emission spectra of EB bound to HS-DNA in the presence of complexes (II). [EB] = 33.3 µM, [DNA] = 10 µM; [complex] = (i) 3.33, (ii) 6.66, (iii) 10, (iv) 13.33, (v) 16.66, (vi) 20, (vii) 23.33, (viii) 26.66, (iX) 30, (X) 33.3 µM; λex= 510 nm. The arrows show the intensity changes upon increasing the concentrations of complex. Inset graph: plots of I_o/I vs. [Q], with • for the experimental data points and the full line for the linear fitting of the data. Comparative plot of log[I_o-I/I] versus log[complex] for the titration of HS-DNA EB system with platinum(II) complexes (II) in phosphate buffer medium.

Pt(L^3)Cl_2] (III)

Volume (μL)	Intensity (CPS) $I_{corr.}$	Intensity (CPS) $I_{obs.}$	I_o/I	$(I_o - I)/I$	$\log(I_o - I/I)$	Q × 10^{-6} (μM)	log Q	K_q (M^{-1})	K_a (M^{-1})	n	ΔG(Jmol^{-1})
0	69224	69086	1.002	0	-	0	-	8.5×10^3	1.32×10^4	0.844	-23,563.19
5	67611	67476	1.025	0.0259	-1.5865	3.33	-5.47712				
10	65935	65803	1.051	0.0519	-1.2841	6.66	-5.17609				
15	64363	64235	1.077	0.077	-1.1097	10	-5				
20	63513	63386	1.092	0.0921	-1.0357	13.3	-4.87506				
25	61185	61063	1.133	0.1336	-0.8740	16.6	-4.77815				
30	59455	59336	1.166	0.1666	-0.7782	20	-4.69897				
35	57824	57709	1.199	0.1995	-0.6999	23.3	-4.63202				
40	57203	57089	1.212	0.2125	-0.6725	26.6	-4.57403				
45	55377	55264	1.252	0.2526	-0.5975	30	-4.52288				
50	53880	53772	1.254	0.2874	-0.5415	33.3	-4.47712				

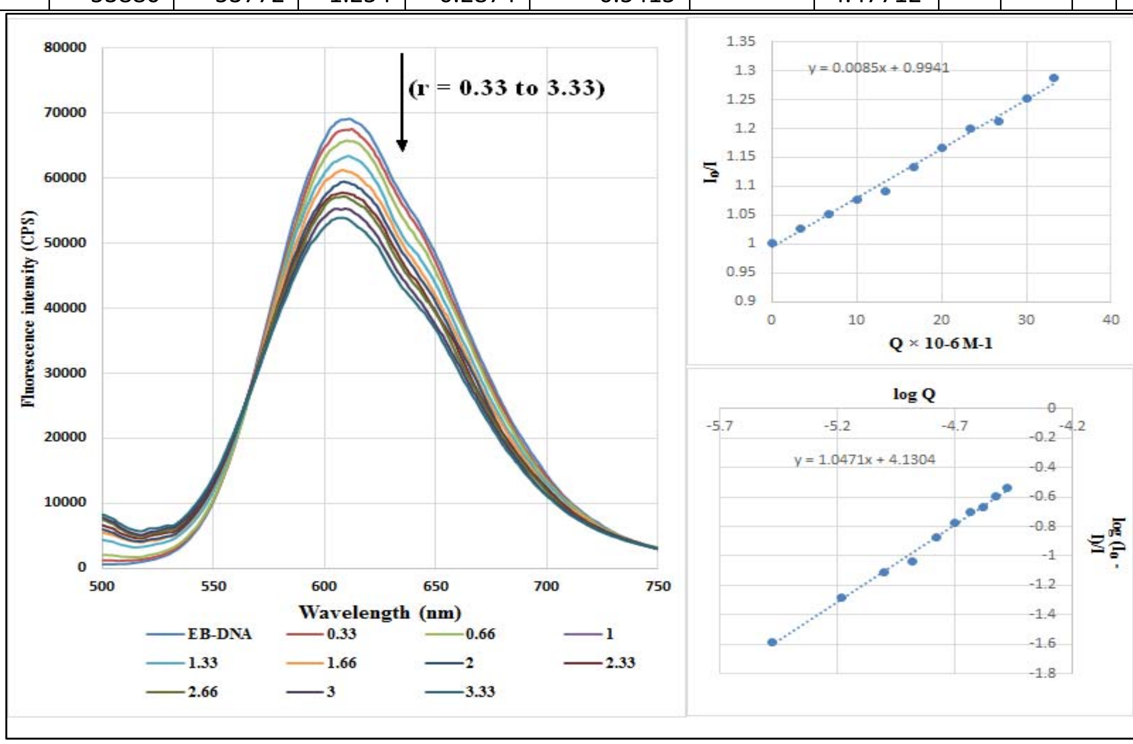

ESI Fig. 3. Fluorescence emission spectra of EB bound to HS-DNA in the presence of complexes (III). [EB] = 33.3 µM, [DNA] = 10 µM; [complex] = (i) 3.33, (ii) 6.66, (iii) 10, (iv) 13.33, (v) 16.66, (vi) 20, (vii) 23.33, (viii) 26.66, (iX) 30, (X) 33.3 µM; λex= 510 nm. The arrows show the intensity changes upon increasing the concentrations of complex. Inset graph: plots of I_o/I vs. [Q], with • for the experimental data points and the full line for the linear fitting of the data. Comparative plot of log[I_o-I/I] versus log[complex] for the titration of HS-DNA EB system with platinum(II) complexes (III) in phosphate buffer medium.

[Pt(L^4)Cl_2] (IV)

Volume (µL)	Intensity (CPS) $I_{corr.}$	Intensity (CPS) $I_{obs.}$	I_o/I	$(I_o - I)/I$	$\log(I_o - I/I)$	Q × 10^{-6} (µM)	log Q	K_q (M^{-1})	K_a (M^{-1})	n	ΔG(J mol^{-1})
0	68566	68430	1.002	0	-	0	-	5.3×10^3	0.77×10^3	0.8153	-16,486.93
5	66706	66573	1.029	0.02994	-1.52375	3.33	-5.47712				
10	65984	65852	1.041	0.04121	-1.38494	6.66	-5.17609				
15	64687	64558	1.062	0.06209	-1.20695	10	-5				
20	63219	63093	1.086	0.08674	-1.06174	13.3	-4.87506				
25	63025	62900	1.090	0.09009	-1.04531	16.6	-4.77815				
30	61852	61729	1.110	0.11077	-0.95558	20	-4.69897				
35	60673	60552	1.132	0.13235	-0.87828	23.3	-4.63202				
40	59743	59624	1.149	0.14997	-0.82398	26.6	-4.57403				
45	59148	59030	1.161	0.16154	-0.79172	30	-4.52288				
50	58034	57918	1.183	0.18385	-0.73552	33.3	-4.47712				

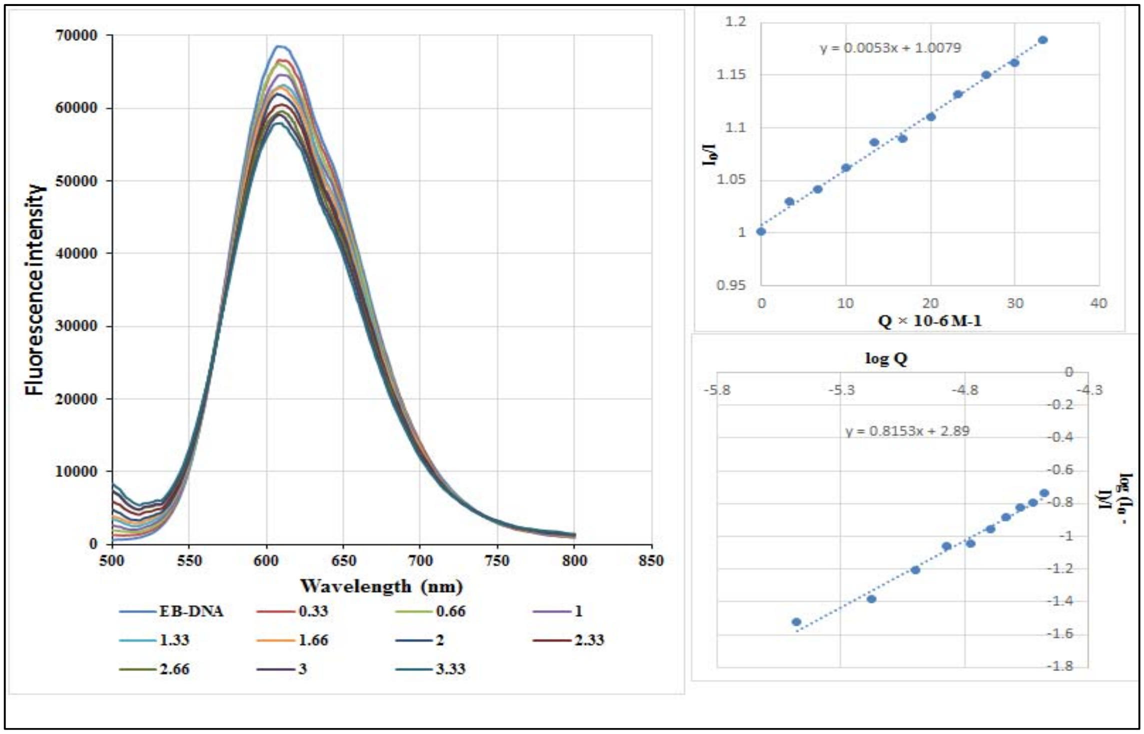

ESI Fig. 4. Fluorescence emission spectra of EB bound to HS-DNA in the presence of complexes (IV). [EB] = 33.3 μM, [DNA] = 10 μM; [complex] = (i) 3.33, (ii) 6.66, (iii) 10, (iv) 13.33, (v) 16.66, (vi) 20, (vii) 23.33, (viii) 26.66, (iX) 30, (X) 33.3 μM; λex= 510 nm. The arrows show the intensity changes upon increasing the concentrations of complex. Inset graph: plots of I_o/I vs. [Q], with • for the experimental data points and the full line for the linear fitting of the data. Comparative plot of log[I_o-I/I] versus log[complex] for the titration of HS-DNA EB system with platinum(II) complexes (IV) in phosphate buffer medium.

$[Pt(L^5)Cl_2]$ (V)

Volume (µL)	Intensity (CPS) $I_{corr.}$	Intensity (CPS) $I_{obs.}$	I_o/I	$(I_o - I)/I$	$\log(I_o - I/I)$	Q × 10^{-6} (µM)	log Q	K_q (M^{-1})	K_a (M^{-1})	n	ΔG (Jmol^{-1})
0	62397	62272	1.002	0	-	0	-	3.3 × 10^2	0.147 × 10^3	0.694	-12,379.45
5	61151	61029	1.022	0.0224	-1.64939	3.33	-5.47712				
10	59929	59810	1.043	0.0432	-1.36393	6.66	-5.17609				
15	59467	59349	1.051	0.0513	-1.28937	10	-5				
20	59440	59321	1.051	0.0518	-1.28531	13.3	-4.87506				
25	58916	58799	1.061	0.0611	-1.21329	16.6	-4.77815				
30	57516	57401	1.087	0.0870	-1.06035	20	-4.69897				
35	57383	57269	1.089	0.0895	-1.04796	23.3	-4.63202				
40	56740	56627	1.101	0.1018	-0.99185	26.6	-4.57403				
45	56718.6	56605	1.102	0.1023	-0.99004	30	-4.52288				
50	55625	55515	1.123	0.1239	-0.90674	33.3	-4.47712				

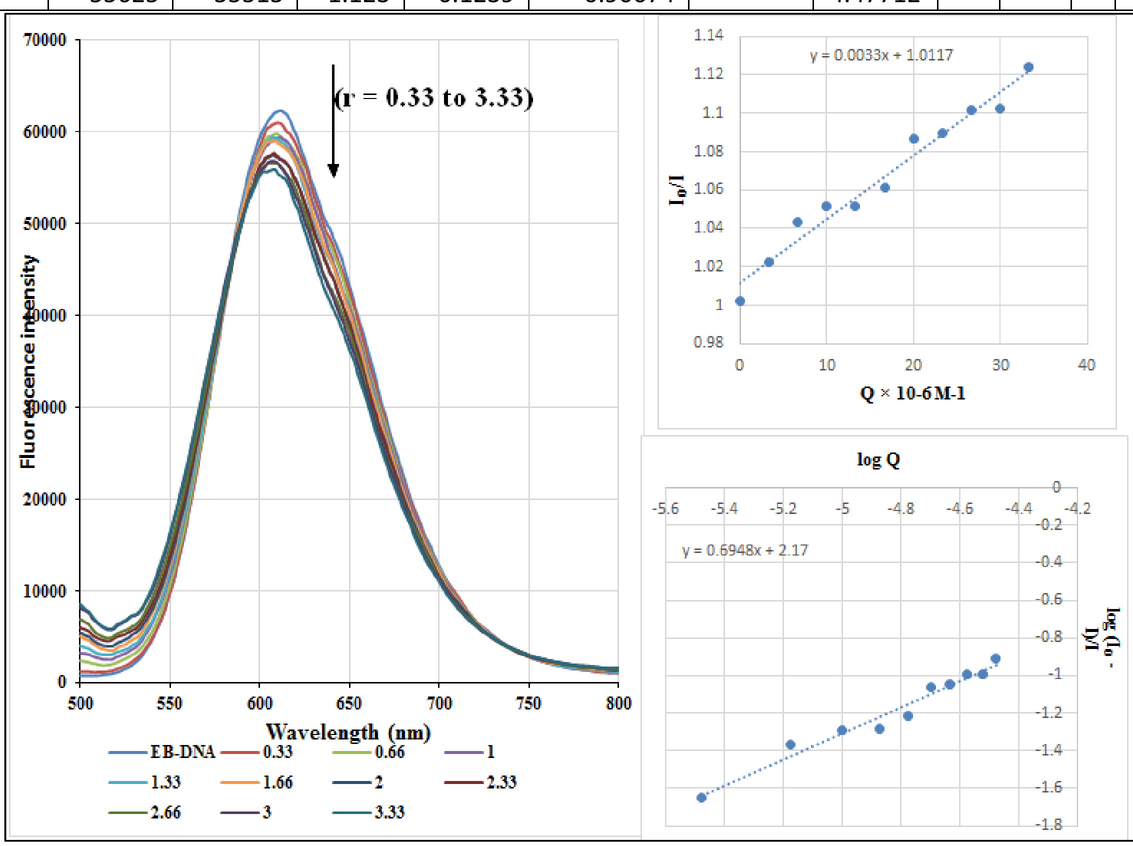

ESI Fig. 5. Fluorescence emission spectra of EB bound to HS-DNA in the presence of complexes (V). [EB] = 33.3 µM, [DNA] = 10 µM; [complex] = (i) 3.33, (ii) 6.66, (iii) 10, (iv) 13.33, (v) 16.66, (vi) 20, (vii) 23.33, (viii) 26.66, (iX) 30, (X) 33.3 µM; λex= 510 nm. The arrows show the intensity changes upon increasing the concentrations of complex. Inset graph: plots of I_o/I vs. [Q], with • for the experimental data points and the full line for the linear fitting of the data. Comparative plot of log[I_o-I/I] versus log[complex] for the titration of HS-DNA EB system with platinum(II) complexes (V) in phosphate buffer medium.

Supplementary material 10: % cleavage ability of the synthesized ligands **(L^1-L^5)** and platinum(II) complexes **(I -V).**

Compounds	OC Form II	SC Form I	% Cleavage
DNA	8.2	91.8	0
K2PtCl4	18.1	81.9	10.78
Cisplatin	90.1	9.9	89.21
Transplatin	58.2	41.8	54.46
L^1	73.8	26.2	71.4
L^2	66.7	33.3	63.72
L^3	70.2	29.8	67.53
L^4	68.2	31.8	65.35
L^5	66	34	62.9
I	89.9	10.1	88.99
II	86.6	13.4	85.4
III	87.9	12.1	86.81
IV	87.3	12.7	86.16
V	85.6	14.4	84.31